The lunar dust environment

Eberhard Grün [a,b,*], Mihaly Horanyi [a], Zoltan Sternovsky [a]

[a] Laboratory for Atmospheric and Space Physics, LASP, University of Colorado, 1234 Innovation Dr. Boulder, CO 80303-7814, USA
[b] Max-Planck-Institut for Nuclear Physics, Saupfercheckweg, D-69117 Heidelberg, Germany

ARTICLE INFO

ABSTRACT

Each year the Moon is bombarded by about 10^6 kg of interplanetary micrometeoroids of cometary and asteroidal origin. Most of these projectiles range from 10 nm to about 1 mm in size and impact the Moon at 10–72 km/s speed. They excavate lunar soil about 1000 times their own mass. These impacts leave a crater record on the surface from which the micrometeoroid size distribution has been deciphered. Much of the excavated mass returns to the lunar surface and blankets the lunar crust with a highly pulverized and "impact gardened" regolith of about 10 m thickness. Micron and sub-micron sized secondary particles that are ejected at speeds up to the escape speed of 2300 m/s form a perpetual dust cloud around the Moon and, upon re-impact, leave a record in the microcrater distribution. Such tenuous clouds have been observed by the Galileo spacecraft around all lunar-sized Galilean satellites at Jupiter. The highly sensitive Lunar Dust Experiment (LDEX) onboard the LADEE mission will shed new light on the lunar dust environment. LADEE is expected to be launched in early 2013.

Another dust related phenomenon is the possible electrostatic mobilization of lunar dust. Images taken by the television cameras on Surveyors 5, 6, and 7 showed a distinct glow just above the lunar horizon referred to as horizon glow (HG). This light was interpreted to be forward-scattered sunlight from a cloud of dust particles above the surface near the terminator. A photometer onboard the Lunokhod-2 rover also reported excess brightness, most likely due to HG. From the lunar orbit during sunrise the Apollo astronauts reported bright streamers high above the lunar surface, which were interpreted as dust phenomena. The Lunar Ejecta and Meteorites (LEAM) Experiment was deployed on the lunar surface by the Apollo 17 astronauts in order to characterize the lunar dust environment. Instead of the expected low impact rate from interplanetary and interstellar dust, LEAM registered hundreds of signals associated with the passage of the terminator, which swamped any signature of primary impactors of interplanetary origin. It was suggested that the LEAM events are consistent with the sunrise/sunset-triggered levitation and transport of charged lunar dust particles. Currently no theoretical model explains the formation of a dust cloud above the lunar surface but recent laboratory experiments indicate that the interaction of dust on the lunar surface with solar UV and plasma is more complex than previously thought.

1. Introduction

Renewed interest in lunar exploration demands an assessment of the potentially hazardous dust environment of the Moon. While not much new observational data has been obtained on the lunar dust environment since the Apollo era, the Galileo mission characterized in detail the dust environment of the similar sized Galilean moons. Also new hypotheses have been developed to explain some of the early enigmatic observations and some novel experiments shed new light on processes that may occur at the lunar surface. The purpose of the paper is to give an up-to-date review of the lunar dust environment and to present an outlook to future research. The paper starts with a brief review of pre-Apollo near-Earth dust measurements and a description of the lunar soil. Section 2 describes the role the lunar microcrater record in deciphering the interplanetary dust flux at 1 AU. The comparison of lunar measurements with results from in-situ dust detectors showed that there is a significant flux of secondary sub-micron sized ejecta particles at the lunar surface that are generated by impact of interplanetary meteoroids. Similar ejecta clouds have been observed around all the Galilean Moons at Jupiter. Section 3 discusses the potential evidence for the lunar dust transport. We conclude with Section 4 with a summary of the outstanding problems in understanding the lunar dust environment and the near future attempts to solve them.

1.1. Early micrometeoroid measurements

Simple but robust micrometeoroid instruments were flown on the first satellites, like on the Explorer 1 satellite. However, because

* Corresponding author at: Max-Planck-Institut for Nuclear Physics, Saupfercheckweg, D-69117 Heidelberg, Germany. Tel.: +49 6221 516478.
E-mail addresses: eberhard.gruen@mpi-hd.mpg.de, eberhard.gruen@lasp.colorado.edu (E. Grün).

of their low sensitivity and small detection area they detected a negligible number of micrometeoroid impacts. More sensitive microphone dust detectors were already flown in 1950 onboard a V2 rocket (Bohn and Nadig, 1950). What the early investigators did not appreciate was the variety of effects that microphones responded to, that were unrelated to dust impacts. Measurements with these instruments resulted in an allegedly high dust flux near Earth. By the analyses of microcraters on lunar samples returned by the Apollo astronauts the controversy was finally settled about the micrometeoroid flux near the Earth and in interplanetary space.

In the early 1960s microphone data with Explorer VIII and some Russian Cosmos satellites were interpreted as near-Earth dust enhancements factors of 1000 and higher than in interplanetary space (Fig. 1). Measurements of the zodiacal light brightness set stringent constraints on the total dust density in interplanetary space (Ingham, 1961). The near-Earth dust enhancement was supported by the first high altitude dust collections using rockets, which found large numbers of particles on the collectors after their return to Earth (Hemenway and Soberman, 1962; Alexander et al., 1963). In a theoretical analysis, Shapiro et al. (1966) concluded that a near-Earth enhancement of at most a factor of 10 could reasonably be explained but not the suggested enhancement factors of 1000 and more. Indeed, the current best estimate of the gravitational enhancement is only a factor 2. Simultaneously, based on the theoretical arguments, Nilsson (1966) expressed "some doubts about the Earth's dust cloud" on experimental grounds. He used witness microphone detectors that were shielded from dust impacts but otherwise identical to the active ones. Both sensors recorded about the same event rate as the active ones and, hence, contradicted the dust enhancement hypothesis. Because of the initial false high flux expectations, subsequent dust detectors and collectors were designed too small and produced no results. Consequently, only upper limits of the dust flux could be established (Fechtig, 1968; Auer et al., 1970). Later, more sophisticated instruments measured similar low fluxes near Earth and in interplanetary space and showed thereby that the initial high fluxes reported were erroneous and caused by the combined effect of immature dust detectors and the harsh near-Earth environment.
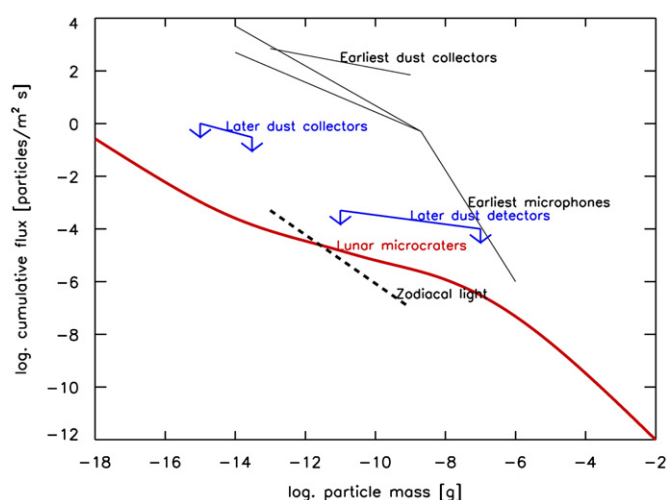
From the beginning of space flight there were engineering type dust experiments that were not designed to address the meteoroid flux as a function of size but to measure only the resulting effects of the dust impacts on space systems. The typical dust detectors were of $1 \, m^2$ area and employed robust detection methods for 100 µm in radius and bigger meteoroids: for example, penetration detectors and capacitor sensors, which were not susceptible to environmental interferences. Detectors of the "beer can"-type were successfully flown on several early satellites and space-probes (e.g. Explorer 16 and 23, Hastings, 1964; O'Neal, 1965). These detectors consisted of a large number of pressurized cells that recorded the decrease in gas pressure that occurred when a 10–20 µm thick wall was punctured by a meteoroid. The Pegasus detectors were large area (about $200 \, m^2$) detectors that recorded penetrations of 40, 200, and 400 µm thick metal foils by the discharge of a capacitor. Detectors like these determined the flux of meteoroids in near-Earth space in the 10 µm to mm size range. This range was important for the assessment of the meteoroid hazard of typical satellites and the manned missions ahead.

It took more than a decade until finally the analyses of the lunar microcrater record reconciled the flux measurements of micron to mm-sized grains at rather low flux levels.

1.2. Lunar soil

The lunar surface is covered by a several meters thick layer of regolith, which overlays the primordial lunar bedrock. Regolith consists of unconsolidated rocks, pebbles, and dust. Most of the regolith is composed of small particles ground down by perpetual meteoroid bombardment. On a global scale, the composition of the lunar regolith is distinguished by the dark basalts of the maria and the lighter-colored feldspar-rich rocks of the lunar highlands. The bulk composition of the lunar soil varies between basaltic and anorthositic. More than a quarter of the lunar soil particles are aggregates of smaller soil particles bonded together by vesicular, flow-banded glass that is created by melting in micrometeoroid impacts (agglutinates), with a smaller fraction of impact-generated glasses and breccias. Breccia is a coarse-grained rock produced in impact fragmentation, composed of angular rock fragments held together by mineral cement or a fine-grained matrix.

The impact processes lead to the shattering, melting, and mixing of the impacted material, creating a layer of weakly cohesive particulate matter. The mean grain size of soil samples returned from the Apollo and Luna programs averages between 60 and 80 µm, but it also includes a significant micron and sub-micron population. The size distribution as well as the layer thickness varies, depending on the landing site, indicating the different ages and length of exposure of the surface to space weathering. Apollo samples revealed the presence of a variety of grain morphologies, from micrometer and sub-micrometer, which agglutinates with irregular and sharp edges to smoother glass droplets of volcanic origins (McKay et al., 1991). In addition, an ultra fine particle content of the regolith ($< 1 \, µm$) was recently found (Greenberg et al., 2007).

2. The lunar micro crater record

2.1. Crater analyses

Impact craters were identified from mm down to sub-micrometer in size on individual rocks (Fig. 2). Several effects, however, impede the comparison of crater distributions on different samples. Since the exposure geometry and time of a given surface

Fig. 1. Development of near-Earth dust flux measurements from 1960 to 1985. Early in-situ dust measurements near-Earth (thin lines and upper limits, Hemenway and Soberman, 1962; Alexander et al., 1963; Fechtig, 1968; Auer et al., 1970) in comparison with interpretations of zodiacal light observations in interplanetary space (dashed line, Ingham, 1961) in comparison with the dust flux derived from lunar microcrater analyses (thick line, Grün et al., 1985). The early dust flux measurements were proved wrong due to insufficient detector technology.
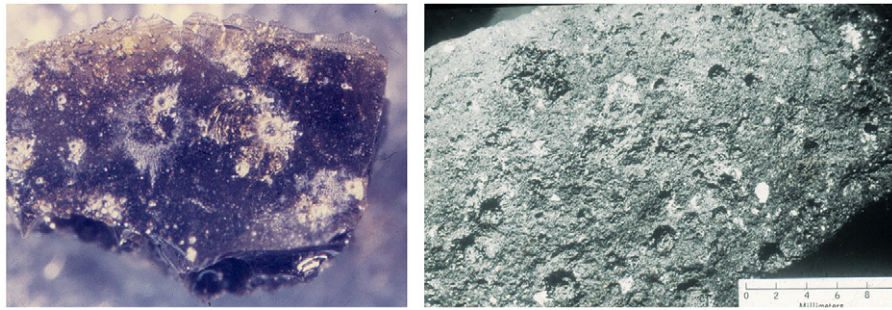
Fig. 2. Lunar samples: glassy sample (left, ca. 10 mm across) displays central pits (dark) surrounded by brighter spallation zones and rocky sample (right, ca. 30 mm across) displays numerous central pits (NASA photos).

on a lunar rock could not be reliably determined, no absolute cratering rates can be derived, but only relative values for different crater sizes.

There were various attempts to determine the lunar microcrater distribution (e.g. Fechtig et al., 1975; Morrison and Zinner, 1977). They differed in the approach how to obtain a distribution over a wide range of crater sizes. While Fechtig et al. combined data from different samples, which individually showed differences in the micron to sub-micron size distribution, Morrison and Zinner (1977) and Morrison and Clanton (1979) obtained a microcrater size-frequency distribution from a single sample (12054, Fig. 3). The slope for small caters (diameter $D < 10\ \mu m$) is smaller for the data of Fechtig et al., than it is for the data of Morrison and Clanton. It has been argued by the latter authors that their data represent the better measure of the primary flux of interplanetary meteoroids because their data need no normalization for different samples and exposure conditions, and because the slope derived for their sizes distribution is the steepest that has been published. That is, they presumed that their sample had been the least affected by shielding from a possible coating of dust on the rocks.

Craters on fragile materials like lunar rocks display a central pit, which is surrounded by a spallation zone from which large chips have been removed (Fig. 2). The ratio of the spallation zone diameter to the central pit diameter is quite variable. Microcraters on lunar rocks have been found ranging from 0.02 μm to mm in diameter. Laboratory simulations of high velocity impacts on lunar-like materials have been used to calibrate crater sizes with projectile sizes and impact speeds. The crater diameter to projectile diameter varies from 2 for the smallest microcraters to about 10 for cm-sized projectiles (Hörz et al., 1975).

The microcrater production rate on a lunar rock is conventionally derived as follows: (1) the surface microcrater density on the rock is measured, (2) the solar flare track "exposure age" of the rock is independently derived, and (3) the crater production rate is then calculated by taking the ratio of (2) over (1). It is assumed that the solar flare track production rate is constant with time. However, the solar flare track production rate may not be reliably determined, since different groups of investigators obtain contradictory results by a factor 50 (Zinner and Morrison, 1976; Hutcheon, 1975; Storzer et al., 1973; Blanford et al., 1975). In addition, it has been argued that the solar flare track production rate could well have been higher about 20,000 years ago than it is today (Zook et al., 1977; Zook, 1980). Such a time variation would give rise to excessive apparent surface exposure ages. All of this experimental evidence led the investigators to the conclusion that lunar rock exposure ages – and microcratering rates – are not reliably obtained from solar flare track data. Therefore, Grün et al. (1985) used in-situ spacecraft measurements to determine the absolute crater production rate and, hence, the meteoroid flux. Of course, this assumes that the size distribution of micrometeoroids
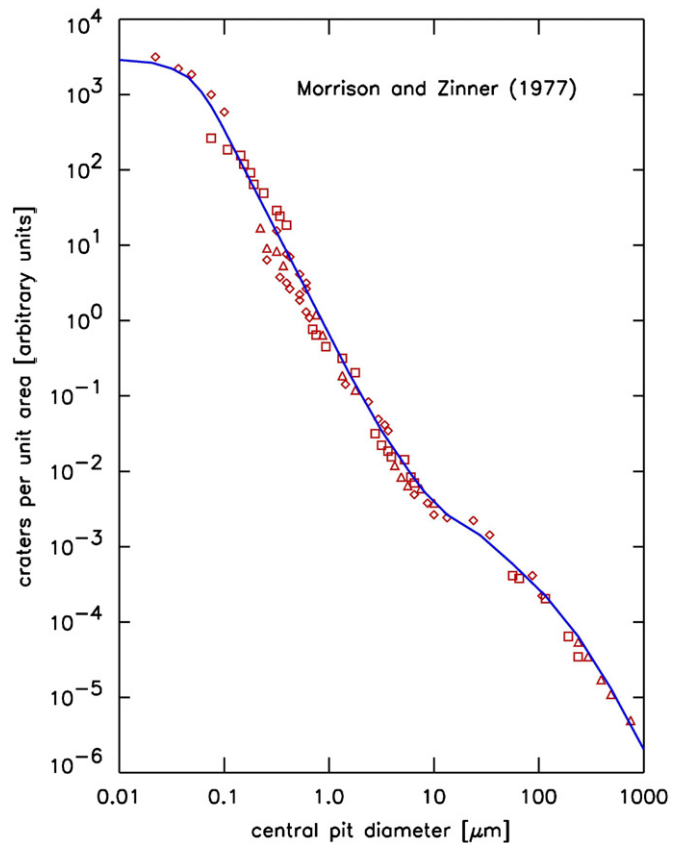

Fig. 3. Crater density on lunar sample 12054. The different symbols refer to various magnifications ranging from 60× to 100 000× at which the sample was analyzed (after Morrison and Zinner, 1977; Morrison and Clanton, 1979).

has not changed much over the last 10^5–10^6 years. Support for this assumption comes from contemporary dust measurements by LDEF over a wide mass range at 1 AU (Love and Brownlee, 1995; McDonnell and Gardner, 1998).

2.2. In-situ detectors

The present day flux of meteoroids at 1 AU has been measured by employing a number of techniques, which include photographic and radar meteor data, in-situ space dust detectors, and space exposed impact sensors—such as spacecraft windows. Impact ionization detectors for the measurement of small ($m < 10^{-12}$ g) particles have been successfully flown as well. An important synthesis and summary of many of the earlier, reliable, data, and their comparison are given by Naumann (1966). Grün et al. (1985) adopted the fit for the Pegasus penetration data that
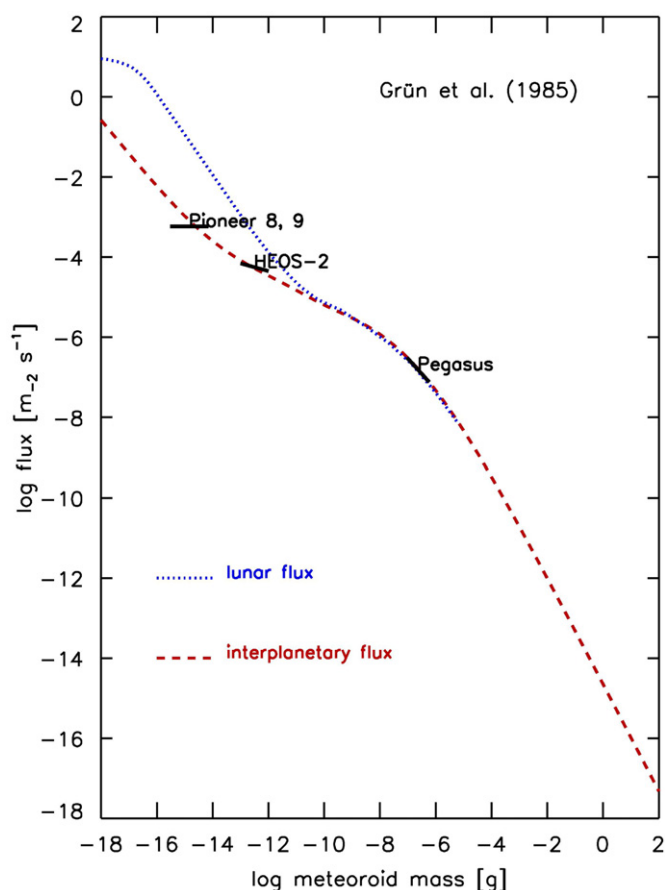
Fig. 4. Interplanetary dust flux (dashed line) and flux at the lunar surface (dotted line, Grün et al., 1985). For the determination of the absolute fluxes spacecraft data have been used (Naumann, 1966; Berg and Grün, 1973; Hoffmann et al., 1975a, b).

were considered highly reliable and well analyzed. These data are representative also of other large meteoroid ($m > 10^{-7}$ g) spacecraft data, which include the Explorer 16 and 23 results, and optical and radar meteor data. Whipple (1967) summarizes several meteor measurements by the dependency of the cumulative flux to be proportional to $m^{-1.34}$. This slope (-1.34) should hold true in the mass range 10^{-4} g $< m < 10^2$ g. The flux distribution derived from the lunar data has exactly this slope for large particles ($m > 10^{-4}$ g). Another set of flux data exists for small meteoroids ($m < 10^{-12}$ g), that is, the flux and anisotropy information of the interplanetary dust from the HEOS-2 (Hoffmann et al., 1975a, b), and from the Pioneer 8 and 9 (Berg and Grün, 1973) dust experiments (Fig. 4).

2.3. Ejecta flux

It was difficult to match the Pioneer 8, 9, HEOS-2 and the Pegasus fluxes to the lunar flux curve. Flavill et al. (1978) and Allison and McDonnell (1981) examined the effects of secondary microcraters produced by ejecta from primary craters on lunar samples. They concluded that secondary microcratering has a significant effect in the 1–10 μm-diameter crater range. The magnitude of the secondary cratering effect depends on the impact geometry. Based on the experimental data available to them (Schneider, 1975; Flavill and McDonnell, 1977), they estimated the number of secondary to primary craters to be of the order of unity in the relevant size range (1–10 μm-diameter crater). Zook et al. (1984) reported results from hypervelocity impact experiments, which showed that the number of secondary

impact pits is more than 2 orders of magnitude higher than was previously thought (Schneider, 1975). The basic difference between these experiments was that the Zook experiments used oblique impact angles in contrast to normal impacts. Since oblique impacts are more realistic for the lunar case, Zook et al. (1984) suggested that "the lunar impact pit population, for pit diameters below about 7 μm, is probably dominated by high-speed secondary ejecta impacts and not by primary meteoroid impacts". Therefore, Grün et al. (1985) concluded that the high-speed ejecta flux at the lunar surface that contributes to the microcrater record is up to two orders of magnitude higher than the interplanetary dust flux for small particles.

2.4. The lunar and interplanetary fluxes

In the analysis of Grün et al. (1985) the following characteristics of the interplanetary meteoroid population have been assumed: (1) the effective meteoroid density is $\rho = 2.5$ g/cm^3, (2) at 1 AU the relative effective speed between different meteoroids as well as the impact speed on the Moon is $v_0 = \sim 20$ km/s, and (3) the flux on the Earth as well as the lunar impact flux is isotropic. The mean spatial mass density is $\sim 10^{-16}$ g/m^3 at 1 AU, and peaks at $m \sim 10^{-5}$ g. Only particles $m > 10^{-10}$ g contribute significantly to the total mass. There is no significant difference between interplanetary and lunar flux curves with respect to the mass distribution. However, there are significant differences with respect to the cross-sectional distributions, which affect the light scattering. The cross-sectional distribution for the lunar flux curve displays two maxima: the larger one at $m \sim 3 \times 10^{-17}$ g and the second at $m \sim 3 \times 10^{-7}$ g. The position of the second peak coincides with the peak of the cross-sectional distribution of the interplanetary flux curve. The color of zodiacal light, which is scattered off interplanetary grains is red (Perrin and Lamy, 1989), whereas light scattered off lunar particles would display a strong UV excess because of the abundance of nanometer sized particles.

Monitoring the near-Earth dust environment is nowadays a routine activity of all major space agencies. In 1984 NASA launched the Long Duration Exposure Facility, LDEF, into near-Earth space at about 450 km altitude. LDEF was designed to study the effects of prolonged exposure to space on various materials. Six years after launch LDEF was retrieved by the Space Shuttle and brought back to the ground. The study of the near-Earth dust environment was also the objective of the European Eureca satellite and of samples from the Russian MIR station, which were returned to Earth. Routine inspections of the Shuttle windows and the solar arrays returned from the Hubble Space Telescope are also used to characterize the damage produced by the meteoroid and debris environment (Humes, 1991; Kinard et al., 1994; Love and Brownlee, 1995; McDonnell and Gardner, 1998; Drolshagen, 2008).

The lunar and near-Earth dust measurements in combination with spacecraft measurements in interplanetary space by the Helios, Galileo, Ulysses, and Cassini spacecraft together with zodiacal light and meteor observations have been used to develop consistent models of the interplanetary dust cloud (Divine, 1993; Staubach et al., 1997; Dikarev et al., 2005).

2.5. Ejecta clouds at the Galilean moons and impact generated dust rings

Evidence for a high secondary particle flux has been observed also at other airless planetary bodies. During its orbit tour about Jupiter, the Galileo spacecraft discovered impact-generated dust clouds surrounding all the Galilean satellites. The impact rate of dust grains showed a sharp peak within about half an hour centered on closest approach to each satellite (Grün et al., 1998;

Krüger et al., 1999), indicating the existence of surrounding dust clouds. These dust clouds are a general phenomenon in the solar system, which has been predicted by modeling and proved by observation (Krüger et al., 2003; Spahn et al., 2006). Particles escaping from the Galilean satellites form a tenuous dust ring in that region. Galileo observed this ring with a peak number density of $5 \times 10^{-7} \, \text{m}^{-3}$ at Europa's orbit (Thiessenhusen et al., 2000; Krivov et al., 2002a). Furthermore, the data indicates an increase in the number density between Europa and Io (Krivov et al., 2002b).

Closer to Jupiter, the small moons Metis, Adrastea, Amalthea, and Thebe act as sources of Jupiter's gossamer ring system via meteoroid impact erosion of their surfaces (Burns et al., 1999). This ring system was investigated with remote imaging from the Earth and by the Voyager, Galileo, Cassini, and New Horizons spacecrafts, revealing a significant structure in the ring. By now, at least four components have been identified (Ockert-Bell et al., 1999; Burns et al., 1999; de Pater et al., 1999): the main ring, interior halo and two gossamer rings. The faint gossamer rings appear to extend primarily inward from the orbits of Amalthea and Thebe. During its last orbits about Jupiter, Galileo made two passages through the gossamer ring system and led to a better understanding of its dust number density and size distribution (Krüger et al., 2009).

It is expected that the Moon has a similar ejecta cloud, although it has not been observed yet, because of the lack of sufficiently sensitive instruments flown in its vicinity. The Lunar Dust EXperiment (LDEX) dust detector onboard the Lunar Dust and Exosphere Explorer (LADEE) mission is to be launched in early 2013 and is expected to remedy this situation (Horanyi et al., 2009).

3. Lunar dust transport

There are several outstanding issues, which must be addressed to ensure acceptable cost and risk for sustained human lunar programs. Arguably, one of the highest-priority issues to be addressed is that of the lunar dust. Fine grains from the surface can be lofted due to human activities, but there is also an evidence that a fraction of the lunar fines is electrostatically charged and naturally transported under the influence of near-surface electric fields. Conjectured resulting transport phenomena range from the levitation of micron size dust grains at low altitudes (centimeter to meter height) to the lofting of sub-micron particles to tens of kilometers. Observations by the Apollo astronauts of sticking of dust to their space suits even after short extravehicular activities demonstrated the importance of control of dust contamination. Simple instruments placed on the lunar surface monitored both natural and man-made dust coverage and cleansing effects that are not fully understood (O'Brien, this issue).

The interaction of the lunar surface with its radiation and plasma environment is expected to be similar to that of an asteroid, Mercury, Mars satellites, Galilean satellites, or a Kuiper Belt Object. Hence the lunar surface offers an excellent laboratory to study processes that could dominate the evolution of surfaces of airless planetary objects throughout the solar system that are directly exposed to plasmas and radiation.

3.1. Horizon glow

Images taken by the television cameras on Surveyors 5, 6, and 7 gave the first indication of dust transport on the airless surface of the Moon (Criswell, 1973; Rennilson and Criswell, 1974). These TV cameras consisted of a vidicon tube, 25–100 mm focal length lenses. Images taken of the western horizon shortly after sunset showed a distinct glow just above the lunar horizon, dubbed horizon glow (HG). This light was interpreted to be forward-scattered sunlight from a cloud of dust particles < 1 m above the surface near the terminator. The HG had a horizontal extent of about 3° on each side of the direction to the Sun (Fig. 5). Assuming that the observed signal is dominated by diffraction and forward scattering of sunlight, this horizontal extent corresponds to spheres of radius ~5 µm for observations at visible wavelengths. Micrometeoroid ejecta, scattering off surface grains, and reflections involving glints off the spacecraft are ruled out by the observed intensity of the signal, its duration (up to 2.5 h), and its vertical and horizontal extent (Rennilson and Criswell, 1974). However, it is difficult to analyze these images. In order to determine the physical dimensions of the bright cloud, the determination of the distance to the cloud is needed. By analyzing the shape of the lower boundary of the Surveyor 7 HG cloud, and matching it to the local topography from orbital photographs of the Surveyor 7 landing site, Rennilson and Criswell (1974) placed the cloud at the visible horizon, or approximately 150 m from the camera. The vertical extent of the cloud is 1.9 mrad or about 30 cm at that distance. Its horizontal extent of 100 mrad makes the observed cloud 14 m wide, though this dimension may be a result of the light scattering properties of the cloud: it could be much larger with the parts of the cloud further from the Sun line not scattering sufficient light into the cameras.

The astrophotometer on the Lunokhod-2 rover also reported excess brightness, most likely due to HG (Severnyi et al., 1975). An independent set of observations related to dust levitation/transport phenomena is the description of the visual observations of the Apollo 17 crew during sunrise as it was seen from the lunar orbit. They reported the appearance of bright streamers with fast temporal brightness changes (seconds to minutes) extending in excess of 100 km above the lunar surface. McCoy and Criswell (1974) argued for the existence of a significant population of lunar particles scattering the solar light. The rough estimates indicated that the scatterers are sub-micron (~0.1 µm) sized
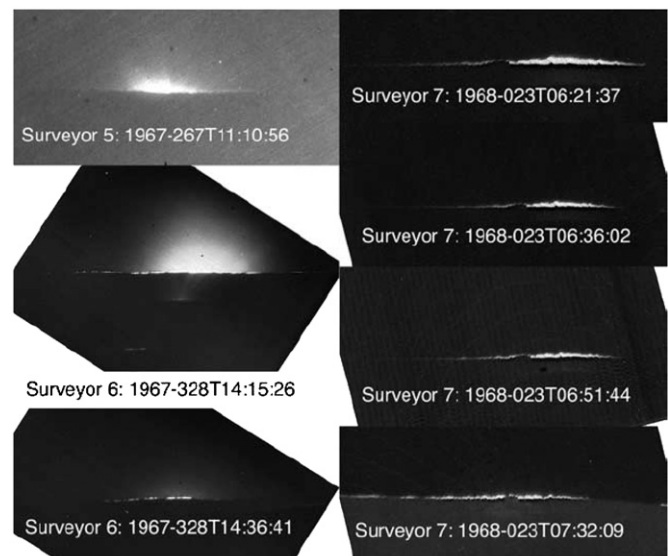

Fig. 5. Surveyor horizon glow (NASA photos, Criswell, 1973; Rennilson and Criswell, 1974; Colwell et al., 2007) is interpreted as forward-scattered sunlight from a cloud of levitated dust particles < 1 m above the surface near the terminator. The horizon glow has a horizontal extent of about 3° on each side of the direction to the Sun. Surveyor 5 and 6 images show significant contributions of zodiacal light that extends higher above the surface.

grains. These drawings were analyzed again (Zook and McCoy, 1991) and most of the earlier conclusions were verified. This study also estimated the scale height of this 'dusty-exosphere' $H\sim10$ km, and suggested that dust levitation could be observed using ground based telescopes. A new simple model suggests that these could be particles with radii <10 nm lofted from the lunar surface by electrostatic forces (Stubbs et al., 2006).

The last set of observations consist of the images taken of the lunar limb by the star tracker camera of the Clementine spacecraft, which showed a faint glow along the lunar surface (Fig. 6), stunningly similar to the sketches of the Apollo 17 astronauts (Science News 3/26/94, H. Zook, private communications, 1994). The interpretation of these images was complicated by the presence of the scattered light from zodiacal dust particles (Hahn et al., 2002), and it was never completed due to the untimely death of H. Zook in 2001.

The discovery of lunar atmospheric sodium and potassium by ground-based observers (Potter and Morgan, 1988) and the in-situ detection of metal ions derived from the Moon in interplanetary space (Mall et al., 1998) stimulated an alternative to levitated dust that is Na D-line emission (Stern, 1999). This idea is pursued by NASA's recent Lunar Reconnaissance Orbiter mission and, especially, by the upcoming LADEE mission.

Fig. 6. Clementine Image of zodiacal light and planets (NASA photo).

3.2. LEAM

The Lunar Ejecta and Meteorites (LEAM) Experiment (Berg et al., 1973) was deployed by the Apollo 17 astronauts on December 11, 1972 in order to characterize the lunar dust environment. It started measurements after the return of the landing module and continued to make observations for about 3 years. The design and the expected performance of the LEAM experiment were similar to the dust experiments onboard the Pioneer 8 and 9 spacecraft that were launched into heliocentric orbits in 1967 and 1968, respectively (Berg and Grün, 1973).

The LEAM instrument consisted of three sensor systems. The EAST sensor was pointed 25° North of East, so that once per lunation its field of view swept into the direction of the interstellar dust flow (Fig. 7). The WEST sensor was pointing in the opposite direction as a control for the EAST sensor, while the UP sensor was parallel to the lunar surface and viewing particles coming from above. Each of these systems was comprised of two sets (front and a back) of 4×4 basic sensor elements to determine the impacting particle's mass, m, and velocity vector, v. The sensors used a combination of thin plastic films and grids to measure the charge from the plasma cloud generated as the dust particles penetrated the film, a signal pulse with amplitude proportional to $m\cdot v^{2.6}$. The two groups of sensors in a system were placed 5 cm apart, and a time-of-flight setup was used to determine the speed of an impacting dust particle. Each of the 16 front sensors were enabled to provide a start signal, and each of the 16 back sensors were designed to provide a stop signal for a total of 256 different combinations, enabling the determination of the velocity vector of the penetrating dust particles. In addition, the back film was attached to a microphone with an acoustic signal proportional to the momentum of the grain. The only exception for this redundant arrangement was the WEST sensor, which lacked a front film. This sensor was designed to identify low-speed ejecta impacts that were expected not to penetrate the front film. Hence, the WEST sensor could not measure particle speed. Extensive laboratory calibrations were performed on these sensors using a 2 MeV electrostatic accelerator with particle masses in the range of $10^{-13}<m<10^{-9}$ g, and velocities up to 25 km/s. The pulse height amplitudes (PHA) from the film-grid sensors were sorted in the (logarithmic) range from 0 to 7.

Once LEAM started to operate it became clear that its observations contradicted expectations. Based on previous measurements in interplanetary space by Pioneer 8 and 9, for example, the
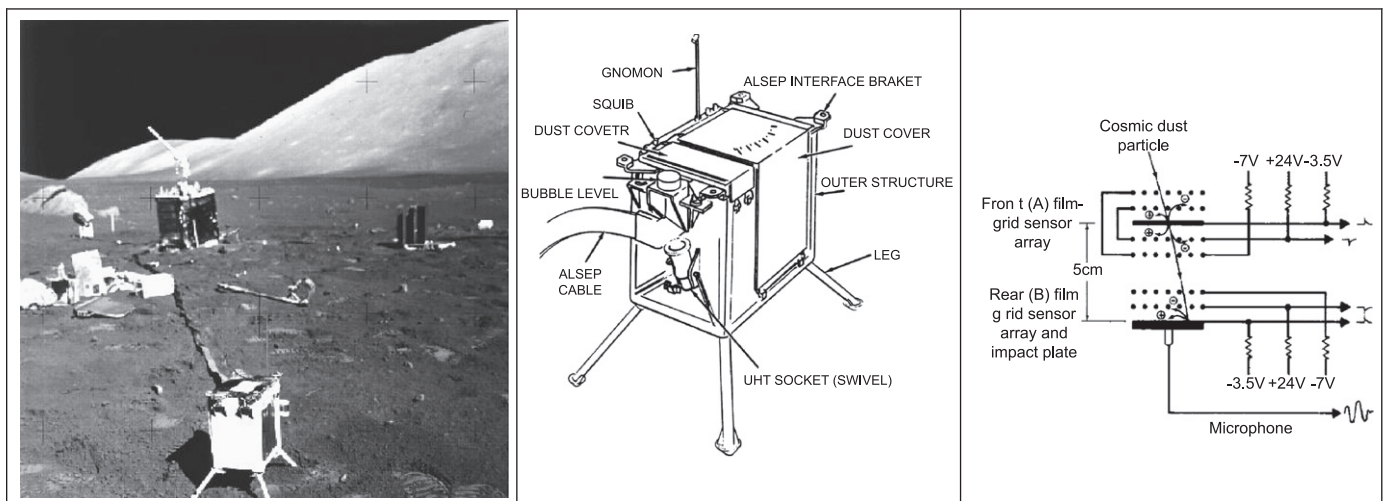

Fig. 7. Apollo 17 ALSEP package with LEAM instrument in the foreground (left, NASA photo) and schematics of LEAM instrument (middle), and one of its basic sensors elements (right) (from: Berg et al., 1973).
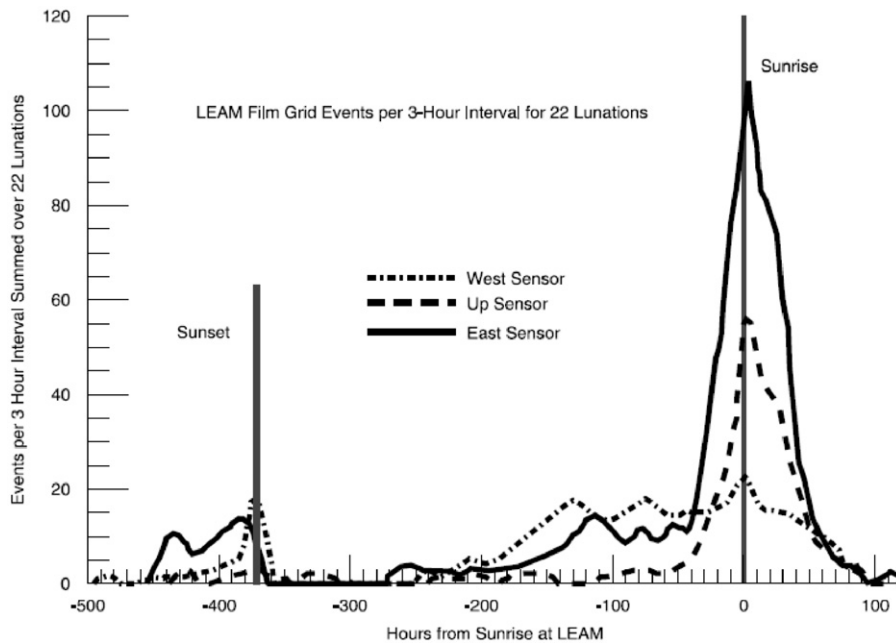
Fig. 8. Number of events recorded by the three LEAM sensors per 3 hour intervals averaged over 22 lunations (Berg et al., 1975). The EAST and WEST sensors measured an approximately constant rate with constant PHA, while the UP sensor registered a declining rate after about 20 months on the lunar surface (O. Berg, personal communication, 2006). From about 100 h after sunrise to about 100 h before sunset the instrument was switched off due to excessive solar heating.

expected impact rate of interplanetary dust particles was a few impact detections per day. Instead, LEAM registered up to hundreds of impacts per day, which swamped any signature of primary impactors of interplanetary or interstellar origin. Most puzzling was the fact that these events registered in the front film only, but frequently with the maximum possible PHA of 7. Additionally, the LEAM operating temperature exceeded its predicted maximum value of $\sim 60\,°C$ at lunar noon, indicating possible thermal problems that were initially believed to be responsible for generating noise in the electronics, and possibly responsible for the elevated impact rates. This was supported by the correlation of the elevated impact rates with the passage of the terminator, both at sunrise and at sunset. As data accumulated, a systematic behavior was recognized. The sunrise terminator event rate started to increase shortly after local midnight at the site, and persisted for a period of approximately 60 h after sunrise—after this time the instrument was switched-off due to excessive solar heating. In this period the rates were up to 100 times higher than the normal background rates (Berg et al., 1975). Fig. 8 shows the number of dust impacts onto LEAM per 3-h period, integrated over 22 lunar days.

A new picture emerged to replace the high temperature electronics explanation: LEAM was registering slow-moving, highly charged lunar dust particles. There were two subsequent studies done to verify this point: a theoretical work to model the response of the electronics (Perkins, 1976), and an experimental study of the LEAM flight spare (Bailey and Frantsvog, 1977). The results of the sensor modeling and circuit analysis showed that charged particles moving at velocities < 1 km/s do produce large PHA responses via induced voltages on the entry grids, as opposed to signals from impact generated plasmas. This explains why the rear films remained silent even though the front sensor seemed to be hit by an energetic dust grain. The experimental study had a similar conclusion: extremely slow moving particles ($v < 100$ m/s) generate a LEAM response up to and including the maximum PHA of 7 if the particles carry a positive charge $Q > 10^{-12}$ C. Both of these studies suggest that the LEAM events are consistent with the sunrise/sunset-triggered levitation and

transport of slow moving, highly charged lunar dust particles. Assuming a daytime surface potential of $+5$ V, the LEAM measurements indicate grains sizes on the order of a millimeter in radius!

4. Outlook

The outstanding issues of the lunar dust environment are the unambiguous detection of electrostatic lofting of dust from the lunar surface and the measurement of the impact ejecta cloud. The existing remote sensing and in-situ observations do not directly prove that the processes leading to dust charging, mobilization, liftoff and transport are active on the Moon. The entire body of these observations is still best explained based on dusty plasma processes at work on the lunar surface. The bombardment and dust ejecta clouds are basic phenomena of the processes in the solar system that have only been observed and characterized for the Galilean Satellites.

Recently, a series of laboratory experiments were conducted to investigate the charging and mobilization of dust under simulated conditions. While it is difficult to reproduce the variable UV and plasma environment of the Moon, these experiments provide insight into the possible physical process responsible for lunar dust transport. The levitation of dust particles in plasma sheaths, where the electrostatic forces balance the gravitational force was achieved by Sickafoose et al. (2002). Dust was observed to collect charge on surfaces exposed to plasma and subsequently transported both horizontally and vertically above an electostatically biased surface that repelled electrons (Wang et al., 2009). Dust was also observed to be transported on surfaces having different secondary electron yields in plasma with an electron beam, as a consequence of differential charging (Wang et al., 2010). Transport by electric fields occurring at electron beam impact/shadow boundaries have been also shown to result in the formation of dust ponds (Wang et al., 2010, this issue).

It is of interest to point out that without localized and probably transient intense electric fields near the lunar surface,

dust particles could not be mobilized. These intense electric fields were shown to develop in the laboratory experiments due to differential charging near UV illumination and/or plasma exposure boundaries, or large gradients in the charging properties of the surface due to changes in its material properties. Similar situations must exist near the lunar terminators, consistent with these laboratory observations.

While ongoing laboratory and remote sensing observations may continue to shed light on dust transport processes, the upcoming LADEE mission will provide a direct assessment of the lunar dust environment. Its instrument payload includes an Ultraviolet Spectrometer (UVS), a Neutral Mass Spectrometer (NMS), and the Lunar Dust Experiment (LDEX). The combination of the UVS remote sensing and the LDEX in-situ dust measurements are expected to characterize the spatial and size distributions of both the impact generated lunar dust "exosphere" as well as the plasma effects induced lofted dust populations, if present.

LDEX is an impact ionization dust detector that is designed based on the HEOS 2, Galileo, Ulysses and Cassini dust instruments. LDEX will detect individual dust grain with mass $m \geq 1.7 \times 10^{-16}$ kg (radius $r_g \geq 0.3$ μm). LDEX will also measure the integrated charge due to grains below the threshold for individual detection, enabling the search for a significant population of grains with $0.1 < r_g < 0.3$ μm over the terminators, indicated by visual observations of Apollo astronauts. The dust detection data will be correlated with the activity of the Sun as electrostatic lofting is expected to depend on the solar UV emission that is highly variable (Sternovsky et al., 2008).

The full understanding of the processes leading to dust transport will require future in-situ dust and plasma measurements on the lunar surface. A possibly autonomously deployed Dusty Plasma Package (DPP) should: (a) determine the charge state, the size and velocity distributions of levitated/transported lunar fines as a function of local time, and position along the lunar orbit; (b) measure the variations of the charge density distribution on the surface, and the plasma properties of the near-surface environment; and (c) map the variable structure of the near-surface electric fields. In addition to lunar science and engineering issues, these measurements are also of great interest in basic plasma as well as general planetary sciences in order to understand the buildup and the collapse of a plasma and photoelectric sheath, and its changing properties with dust loading, possibly leading to dust charging, mobilization, and transport on all airless bodies in the solar system.

References

Alexander, W.M., McCracken, C.W., Secretan, L., Berg, O.E., 1963. Review of direct measurements of interplanetary dust from satellites and probes, Space Research III, 891. North-Holland Publishing Company, Amsterdam.

Allison, R.J., McDonnell, J.A.M., 1981. Secondary cratering-effects on lunar microterrain: implications for the micrometeoroid flux. Proc. Lunar Planet. Sci. Conf 12B, 1703–1716.

Auer, S., Fechtig, H., Feuerstein, M., Gerloff, U., Rauser, P., Weihrauch, J., 1970. Rocket experiments using extremely sensitive detectors for cosmic dust particles, Space Research X, 287. North-Holland Publishing Company, Amsterdam.

Bailey, C.L., Frantsvog, D.J., 1977. Response of the LEAM detector to positively charged microparticles. Concordia College (NASA Contract No. NAS5-23557).

Berg, O.E., Richardson, F.F., Burton, H., 1973. Lunar Ejecta an Meteorites Experiment, in: APOLLO 17 Preliminary Science Report, NASA SP-330, 16.

Berg, O.E., Grün, E., 1973. Evidence of hyperbolic cosmic dust particles. Space Res. XIII 2, 1047–1055.

Berg, O.E., Wolf, H., Rhee, J.W., 1975. Lunar soil movement registered by the Apollo 17 cosmic dust experiment, in: Interplanetary Dust and Zodiacal Light, Lecture Notes in Physics 48, 233.

Blanford, G.E., Fruland, R.M., Morrison, D.A., 1975. Long-term differential energy spectrum for solar-flare iron-group particles, in: Proceedings of the Lunar Science Conference, 6th 3, 3557–3576.

Bohn, J.L., Nadig, F.H., 1950. Researches in the physical properties of the upper atmosphere with special emphasis on acoustical studies with V-2 rockets. Research Institute of Temple University, Report No. 8, pp. 1–26.

Burns, J.A., Showalter, M.R., Hamilton, D.P., Nicholson, P.D., de Pater, I., Ockert-Bell, M.E., Thomas, P.C., 1999. The formation of Jupiter's faint rings. Science 284, 1146–1150.

Colwell, J.E., Batiste, S., Horányi, M., Robertson, S., Sture, S., 2007. The lunar surface: dust dynamics and regolith mechanics. Rev. Geophys. 45 (2). doi:10.1029/2005RG000184.

Criswell, D.R., 1973. Horizon-glow and the motion of lunar dust. In: Grard, R.J.L. (Ed.), Photon and Particle Interaction in Space. D Reidel, Dordrecht, pp. 545.

de Pater, I., Showalter, M.R., Burns, J.A., Nicholson, P.D., Liu, M.C., Hamilton, D.P., Graham, J.R., 1999. Keck infrared observations of Jupiter's ring system near Earth's 1997 ring plane crossing. Icarus 138, 214–223.

Dikarev, V., Grün, E., Baggaley, J., Galligan, D., Landgraf, M., Jehn, R., 2005. The new ESA meteoroid model. Adv. Space Res. 35, 1282–1289.

Divine, N., 1993. Five populations of interplanetary meteoroids. J. Geophys. Res. 98, 17029–17048.

Drolshagen, G., 2008. Impact effects from small size meteoroids and space debris. Adv. Space Res. 41 (7), 1123–1131.

Fechtig, H., 1968. Die Konzentration des Kosmischen Staubes in Erdnähe. Mitteilungen der Astronomischen Gesellschaft 25 65 e.

Fechtig, H., Gentner, W., Hartung, J.B., Nagel, K., Neukum, G., Schneider, E., Storzer, D., 1975. Microcraters on lunar samples, in: Proceedings of the Soviet American Conference on Cosmochem. Moon Planets, NASA-SP-370, pp. 585–603.

Flavill, R.P., Allison, R.J., McDonnell, J.A.M., 1978. Primary, secondary and tertiary microcrater populations on lunar rocks: effects of hypervelocity impact microejecta on primary population, in: Proceedings of the Lunar and Planetary Science Conference, 9th, pp. 2539–2556.

Flavill, R.P., McDonnell, J.A.M., 1977. Laboratory simulation of secondary lunar microcraters from micron scale hypervelocity impacts on lunar rock. Meteoritics 12, 220–225.

Greenberg, P.S., Chen, D., Smith, S.A., 2007. Aerosol Measurements of the Fine and Ultrafine Particle Content of Lunar Regolith, NASA/TM-2007-214956.

Grün, E., Zook, H.A., Fechtig, H., Giese, R.H., 1985. Collisional balance of the meteoritic complex. Icarus 62, 244–272.

Grün, E., Krüger, H., Graps, A., Hamilton, D.P., Heck, A., Linkert, G., Zook, H., Dermott, S.F., Fechtig, H., Gustafson, B., Hanner, M., Horanyi, M., Kissel, J., Lindblad, B., Linkert, G., Mann, I., McDonnell, J.A.M., Morfill, G.E., Polanskey, C., Schwehm, G.H., Srama, R., 1998. Galileo observes electromagnetically coupled dust in the Jovian magnetosphere. J. Geophys. Res. 103, 20011–20022.

Hahn, J.M., Zook, H.A., Cooper, B., Sunkara, B., 2002. Clementine observations of the zodiacal light and the dust content of the inner solar system. Icarus 158, 360–378.

Hastings, E.C. Jr., Ed., 1964, NASA TM X-949, March 1964.

Hemenway, C.L., Soberman, R.K., 1962. Symposium: small meteoric particles in the earth's neighborhood: studies of micrometeorites obtained from a recoverable sounding rocket. Astronom. J. 67, 256.

Hoffmann, H.-J., Fechtig, H., Grün, E., Kissel, J., 1975a. First results of the micrometeoroid experiment S-215 on HEOS 2 Satellite. Planet. Space Sci. 23, 215–224.

Hoffmann, F.-J., Fechtig, H., Grün, E., Kissel, J., 1975b. Temporal fluctuations and anisotropy of the micrometeoroid flux in the Earth—Moon system. Planet. Space Sci. 23, 985–991.

Horanyi, M., Sternovsky, Z., Gruen, E., Srama, R., Lankton, M., Gathright, D., 2009. The Lunar Dust EXperiment (LDEX) on the Lunar Atmosphere and Dust Environment Explorer (LADEE) Mission, Lunar and Planetary Institute Science Conference Abstracts, 40, 1741.

Hörz, F., Brownlee, D.E., Fechtig, H., Hartung, J.B., Morrison, A., Neukum, G., Schneider, E., Vedder, J.F., Gault, D.E., 1975. Lunar microcraters: implications for the micrometeoroid complex. Planet. Space Sci. 23, 151–172.

Humes, D.H., 1991. Large Craters on the Meteoroid and Space Debris Impact Experiment. In: Levine, Arlene S. (Ed.), LDEF, 69 months in space: first post-retrieval symposium. National Aeronautics and Space Administration, 1991, Office of Management, Scientific and Technical Information Program, Washington, D.C., p. 399.

Hutcheon, I.D., 1975. Micrometeorites and solar flare particles in and out of the ecliptic. J. Geophys. Res. 80, 4471–4483.

Ingham, M., 1961. The nature and distribution of the interplanetary dust. M. N. Roy. Ast. Soc. 122, 157.

Kinard, W., O'Neal, R., Wilson, B., Jones, J., Levine, A., Calloway, R., 1994. Overview of the space environmental effects observed on the retrieved long duration exposure facility (LDEF). Adv. Space Res. 14 (10), 7–16.

Krivov, A.V., Krüger, H., Grün, E., Thiessenhusen, K.-U., Hamilton, D.P., 2002a. A tenuous dust ring of Jupiter formed by escaping ejecta from the Galilean satellites. J. Geophys. Res., 107:E1. doi:10.1029/2000JE001434.

Krivov, A.V., Krüger, H., Grün, E., Thiessenhusen, K.-U., Hamilton, D.P., 2002b. A tenuous dust ring of Jupiter formed by escaping ejecta from the Galilean satellites. J. Geophys. Res. (Planets) 107, 5002.

Krüger, H., Krivov, A.V., Hamilton, D.P., Grün, E., 1999. Detection of an impact-generated dust cloud around Ganymede. Nature 399, 558–560.

Krüger, H., Krivov, A.V., Sremcevic, M., Grün, E., 2003. Impact-generated dust clouds surrounding the Galilean moons. Icarus 164, 170–187.

Krüger, H., Hamilton, D.P., Moissl, R., Grün, E., 2009. Galileo in-situ dust measurements in Jupiter's gossamer rings. Icarus 203, 198–213.

Love, S.G., Brownlee, D.E., 1995. A direct measurement of the terrestrial mass accretion rate of cosmic dust. Science 262, 550–553.

Mall, U., Kirsch, E., Cierpka, K., Wilken, B., Söding, A., Neubauer, F., Gloeckler, G., Galvin, A., 1998. Direct observation of lunar pick-up ions near the Moon. Geophys. Res. Lett. 25, 3799–3802.

McCoy, J.E., Criswell, D.R., 1974. Evidence for a high latitude distribution of lunar dust. in: Proceedings of the Fifth Lunar Conference, vol. 3, p. 2991.

McDonnell, J.A.M., Gardner, D.J., 1998. Meteoroid morphology and densities: decoding satellite impact data. Icarus 133, 25–35.

McKay, D.S., Heiken, G., Basu, A., Blanford, G., Simon, S., Reedy, R., French, B.M., Papike, J., 1991. In: Heiken, G., Vaniman, D.T., French, B.M. (Eds.), The Lunar Regolith, in the Lunar Sourcebook. Cambridge Univ. Press, New York, pp. 285–356.

Morrison, D.A., Clanton, U.S. 1979. Properties of microcraters and cosmic dust of less than 1000 Å dimensions. in: Proceedings of the Lunar and Planetary Science Conference, l0th, pp. 1649–1663.

Morrison, D.A., and E. Zinner. 1977. 12054 and 76215: New measurements of interplanetary dust and solar flare fluxes. in: Proceedings of Lunar Science Conference, 8th, pp. 841–863.

Naumann, R.J., 1966. The near Earth Meteoroid Environment. NASA TND 3717.

Nilsson, C., 1966. Some doubts about the Earth's dust cloud. Science 153, 1242–1246.

O'Brien, B., Review of measurements of dust movements on the Moon during Apollo. Planet. Space Sci., this issue. doi:10.1016/j.pss.2011.04.016.

Ockert-Bell, M.E., Burns, J.A., Daubar, I.J., Thomas, P.C., Veverka, J., Belton, M.J.S., Klaasen, K.P., 1999. The structure of Jupiter's ring system as revealed by the Galileo imaging experiment. Icarus 138, 188–213.

O'Neal, R.L., 1965. Ed., NASA TM X-1123, August 1965.

Perkins, D., 1976. Analysis of the LEAM experiment response to charged particles, Bendix Aerospace systems Division, BSR 4233 (NASA Contract no. NAS9-14751).

Perrin, J.M., Lamy, P.L., 1989. Infrared properties of rough cometary grains. Adv. Space Res. 9, 241–246.

Potter, A.E., Morgan, T.H., 1988. Discovery of sodium and potassium vapor in the atmosphere of the moon. Science 241, 675–680.

Rennilson, J.J., Criswell, D.R., 1974. Surveyor observations of lunar horizon glow. The Moon 10, 121.

Schneider, E., 1975. Impact ejecta exceeding lunar escape velocity. Moon 13, 173–184.

Severnyi, A.B., Terez, E.I., Zvereva, A.M., 1975. The measurements of sky brightness on Lunokhod-2. The Moon 14, 123–128.

Shapiro, I.C., Lautman, D.A., Colombo, G., 1966. The earth's dust belt: fact or fiction? 1. Forces perturbing dust particle motion. J. Geophys. Res. 71, 5695–5704.

Sickafoose, A.A., Colwell, J.E., Horanyi, M., Robertson, S., 2002. Experimental levitation of dust grains in a plasma sheath. J. Geophys. Res. 107 (A11), 1408.

Spahn, Frank, Jürgen, Schmidt, Nicole, Albers, Marcel, Hörning, Martin, Makuch, Martin, Seiß, Sascha, Kempf, Ralf, Srama, Valeri, Dikarev, Stefan, Helfert, Georg, Moragas-Klostermeyer, Alexander V., Krivov, Miodrag, Sremcevic, Anthony J., Tuzzolino, Thanasis, Economou, Grün, Eberhard, 2006. Cassini dust measurements at enceladus and implications for the origin of the E ring. Science 311 (5766), 1416. doi:10.1126/science.1121375.

Staubach, P., Grün, E., Jehn, R., 1997. The meteoroid environment near earth. Adv. Space Res. 19, 301–308.

Stern, S.A., 1999. The lunar atmosphere: history, status, current problems, and context. Rev. Geophys. 37, 453–492.

Sternovsky, Z., Chamberlin, P., Horanyi, M., Robertson, S., Wang, X., 2008. Variability of the lunar photoelectron sheath and dust mobility due to solar activity. J. Geophys. Res. 113, A10104. doi:10.1029/2008JA013487.

Storzer, D., Poupeau, G., Kreätschmer, W., 1973. Track-exposure and formation ages of some lunar samples. in: Proceedings of the Lunar Science Conference, 4th 3, pp. 2363–2377.

Stubbs, T.J., Vondrak, R.R., Farrell, W.M., 2006. A dynamic fountain model for lunar dust. Adv. Space Res. 37, 59–66.

Thiessenhusen, K.-U., Krüger, H., Spahn, F., Grün, E., 2000. Dust grains around Jupiter—the observations of the Galileo dust detector. Icarus 144, 89–98.

Wang, X., Horányi, M., Robertson, S., 2009. Experiments on dust transport in plasma to investigate the origin of the lunar horizon glow. J. Geophys. Res. 114, A05103. doi:10.1029/2008JA013983.

Wang, X., Horányi, M., Robertson, S., 2010. Investigation of dust transport on the lunar surface in a laboratory plasma with an electron beam. J. Geophys. Res 15, 11102. doi:10.1029/2010JA015465.

Wang, X., Horányi, M., Robertson, S., Dust transport near electron beam impact and shadow boundaries, Planet. Space Sci., this issue. doi:10.1016/j.pss.2010.12.005.

Whipple, F.L., 1967. On maintaining the meteoritic complex. In: Zodiacal Light and the Interplanetary Medium, NASA-SP 150, pp. 409–426.

Zinner, E., Morrison, D.A., 1976. Comment on "Micrometeorites and Solar Flare Particles in and out of the Ecliptic," by 1. D. Hutcheon. J. Geophys. Res. 81, 6364–6366.

Zook, H.A., Hartung, J.B., Storzer, D., 1977. Solar flare activity: evidence for large-scale changes in the past. Icarus 32, 106–126.

Zook, H.A., 1980. On lunar evidence for a possible large increase in solar flare activity—2×10^4 years ago. In: Pepin, R.O., Eddy, J.A., Merrill, R. (Eds.), Proc. Conf. Ancient Sun, pp. 245–266.

Zook, H.A., Lange, G., Grün, E., Fechtig, H., 1984. Lunar primary and secondary microcraters and the micrometeoroid flux. Lunar Planet. Sci. XV, 965–966.

Zook, H.A., McCoy, E., 1991. Large scale lunar horizon glow and a high altitude lunar dust exosphere. GRL 18, 2117.